The temperature of Europe during the Holocene reconstructed from pollen data

B.A.S. Davis[a,b,*], S. Brewer[b], A.C. Stevenson[a], J. Guiot[c], Data Contributors[1]

[a] *Department of Geography, University of Newcastle, Newcastle upon Tyne, NE1 7RU, UK*
[b] *IMEP, CNRS UPRES A6116, Faculté de St Jérôme, Case 451, 13397 Marseille, Cedex 20, France*
[c] *CEREGE, Europôle de l'Arbois, B.P. 80, 13545 Aix-en-Provence, Cedex 04, France*

Abstract

We present the first area-average time series reconstructions of warmest month, coldest month and mean annual surface air temperatures across Europe during the last 12,000 years. These series are based on quantitative pollen climate reconstructions from over 500 pollen sites assimilated using an innovative four-dimensional gridding procedure. This approach combines three-dimensional spatial gridding with a fourth dimension represented by time, allowing data from irregular time series to be 'focussed' onto a regular time step. We provide six regional reconstructed temperature time series as well as summary time series for the whole of Europe. The results suggest major spatial and seasonal differences in Holocene temperature trends within a remarkably balanced regional and annual energy budget. The traditional mid-Holocene thermal maximum is observed only over Northern Europe and principally during the summer. This warming was balanced by a mid-Holocene cooling over Southern Europe, whilst Central Europe occupied an intermediary position. Changes in annual mean temperatures for Europe as a whole suggest an almost linear increase in thermal budget up to 7800 BP, followed by stable conditions for the remainder of the Holocene. This early Holocene warming and later equilibrium has been mainly modulated by increasing winter temperatures in the west, which have continued to rise at a progressively decreasing rate up to the present day.
© 2003 Elsevier Ltd. All rights reserved.

1. Introduction

A number of attempts have recently been made to develop dynamic regional and global time series temperature reconstructions for the last 1000 years (Mann et al., 1999; Shaopeng et al., 2000; Briffa et al., 2001). These reconstructions have been used to investigate the role of various natural and anthropogenic forcing on the climate system, and the ability of climate models to reproduce them (Jones et al., 1998). The

*Corresponding author. Tel.: +44-(0)-191-2226359; fax: +44-(0)-191-2225421.

E-mail address: basil.davis@ncl.ac.uk (B.A.S. Davis).

[1] The data contributors have all provided pollen data for this study. The subsequent analysis and interpretation is the work and responsibility of the first four authors. The contributors include: Allen, J., Almqvist-Jacobson, H., Ammann, B., Andreev, A.A., Argant, J., Atanassova, J., Balwierz, Z., Barnosky, C.D., Bartley, D.D., Beaulieu, JL de, Beckett, S.C., Behre, K.E., Bennett, K.D., Berglund, B.E.B., Beug, H-J., Bezusko, L., Binka, K., Birks, H.H., Birks, H.J.B., Björck, S., Bliakhartchouk, T., Bogdel I., Bonatti, E., Bottema, S., Bozilova, E.D.B., Bradshaw, R., Brown, A.P., Brugia-paglia, E., Carrion, J., Chernavskaya, M., Clerc, J., Clet, M., Coûteaux, M., Craig, A.J., Cserny, T., Cwynar, L.C., Dambach, K., De Valk, E.J., Digerfeldt, G., Diot, M.F., Eastwood, W., Elina, G., Filimonova, L., Filipovitch, L., Gaillard-Lemdhal, M.J., Gauthier, A., Göransson, H., Guenet, P., Gunova, V., Hall, V.A.H., Harmata, K., Hicks, S., Huckerby, E., Huntley, B., Huttunen, A., Hyvärinen, H., Ilves, E., Jacobson, G.L., Jahns, S., Jankovská, V., Jóhansen, J., Kabailiene, M., Kelly, M.G., Khomutova, V.I., Königsson, L.K.,

Kremenetski, C., Kremenetskii, K.V., Krisai, I., Krisai, R., Kvavadze, E., Lamb, H., Lazarova, M.A., Litt, T., Lotter, A.F., Lowe, J.J., Magyari, E., Makohonienko, M., Mamakowa, K., Mangerud, J., Mariscal, B., Markgraf, V., McKeever, Mitchell, F.J.G., Munuera, M., Nicol-Pichard, S., Noryskiewicz, B., Odgaard, B.V., Panova, N.K., Pantaleon-Cano, J., Paus, A.A., Pavel, T., Peglar, S.M., Penalba, M.C., Pennington, W., Perez-Obiol, R., Pushenko, M., Ralska-Jasiewiszowa, M., Ramfjord, H., Regnéll, J., Rybnickova, E., Rybnickova, M., Saarse, L., Sanchez Gomez, M.F., Sarmaja-Korjonen, K., Sarv, A., Seppa, H., Sivertsen, S., Smith, A.G., Spiridonova, E.A., Stancikaite, M., Stefanova, J., Stewart, D.A., Suc, J-P., Svobodova, H., Szczepanek, K., Tarasov, P., Tobolski, K., Tonkov, Sp., Turner, J., Van der Knaap, W.O., Van Leeuwen, J.F.N., Vasari, A., Vasari, Y., Verbruggen, C., Vergne, V., Veski, S, Visset, L., Vuorela, I., Wacnik, A., Walker, M.J.C., Waller, M.P., Watson, C.S., Watts, W.A., Whittington, G., Willis, K.J., Willutzki, H., Yelovicheva, Ya., Yll, E.I., Zelikson, E.M., Zernitskaya, V.P.

development of these time series has mainly been based on annually resolved proxies, particularly tree-rings, effectively limiting such studies to the last millennia when annual archives are widely available. On longer time scales, non-annually resolved proxies such as pollen data occur more extensively, but the problem of chronological control has led to the adoption of a different non-dynamic approach to regional synthesis. Typically, these have been based on a broad time slice with samples assimilated within a 500–1000-year time window around the target time, such as the 'mid-Holocene' 6000 ± 500 years ^{14}C BP (COHMAP Members, 1988; Huntley and Prentice, 1993; Cheddadi et al., 1997). These static map-based reconstructions have been widely applied to data-model comparisons using climate models run to equilibrium (Prentice et al., 1997; Masson et al., 1999).

As computing power continues to increase, then standard models (AGCMs/CGCMs) can be run for progressively longer periods. Also, a new type of climate model has recently been developed called Earth system models of intermediate complexity (EMICs) (Claussen et al., 2002) which allow the simulation of climate over much longer time periods, including the whole Holocene (Crucifix et al., 2002). These allow the dynamic time-dependent response of the atmosphere to be investigated against a variety of internal (ice, ocean circulation, biosphere, trace gases) and external (orbital) forcing mechanisms (Brovkin et al., 1999; Ganopolski and Rahmstorf, 2001; Weber, 2001). Evaluation of these model simulations against actual climate change requires palaeoclimate data at a comparable temporal and spatial scale. This requires not only a long-term (Holocene) time frame and grid-box (continental) scale, but also a dynamic approach that allows data-model comparison through time.

In this study, we present an innovative new approach to non-annual (pollen-based) palaeoclimate data assimilation and presentation that provides a dynamic and quantitative view of Continental-scale climate change compatible with climate model output. This approach uses a new four-dimensional gridding procedure to assimilate data from hundreds of sites and thousands of samples onto a regular spatial grid and time step. We have applied this method to a palaeo-temperature dataset derived from pollen samples from sites across Europe. This dataset was created using an improved modern-analogue pollen-climate transfer function that can accommodate non-analogous fossil pollen assemblages. The reconstructions include seasonal (coldest month/warmest month) and annual mean temperatures, providing an all-year perspective on temperature trends. We present the results as area-average time series calculated for the whole of Europe and six sub-regions at a 100-year pseudo-resolution (time step) over the last 12,000 years.

2. Data

2.1. Modern pollen data and climate

The modern pollen surface sample dataset used in the transfer function consisted of 2363 samples from throughout North Africa and Europe west of the Urals. This was based on data from the European Pollen Database (EPD), the authors, the PANGAEA data archive, H.J.B. Birks and S. Peglar. All samples were composed of original raw counts of the full assemblage. Each sample site was assigned a modern climate based on interpolation from station data using an artificial neural network (Guiot et al., 1996).

2.2. Fossil pollen data and age-depth modelling

The fossil pollen dataset consisted of 510 selected cores from the EPD and PANGAEA data archive, supplemented by additional data from the authors and individual contributors (Fig. 1a). All samples from these cores consisted of original counts based on the full assemblage. Only cores with absolute dating control were included (radiocarbon, annual laminations, etc.), except where an alternative chronology was suggested by the original author, or where a clear stratigraphic correlation could be made with an independently dated adjacent core. Age-depth models were created for each core based on a calibrated radiocarbon time-scale. Radiocarbon dates were calibrated using the OXCAL3.5 program (Bronk Ramsey, 2000). All ages quoted are in calendar years BP (1950). The choice of age-depth model follows that of the original author where this has been published or provided with the data. For other cores, the most appropriate model was fitted (linear, polynomial, etc.) based on the chronological control points and any additional published information. The control points used for each of the cores is shown in Fig. 1c. Age control for the dataset is based on over 2000 radiocarbon dates and 680 other absolute dates.

3. Methods

3.1. Pollen-climate reconstruction

Fossil pollen samples were assigned a palaeoclimate using a modern analogue matching technique based on a training set of modern pollen samples (Guiot, 1990). This method has been employed in a large number of studies at both single site (Cheddadi et al., 1998) and continental (Cheddadi et al., 1997) scales, and is discussed in detail in many previous papers (e.g. Magny et al., 2001). In this study we have applied a modification to the technique, using PFT (Plant Functional Type) scores (Prentice et al., 1996) to match the fossil
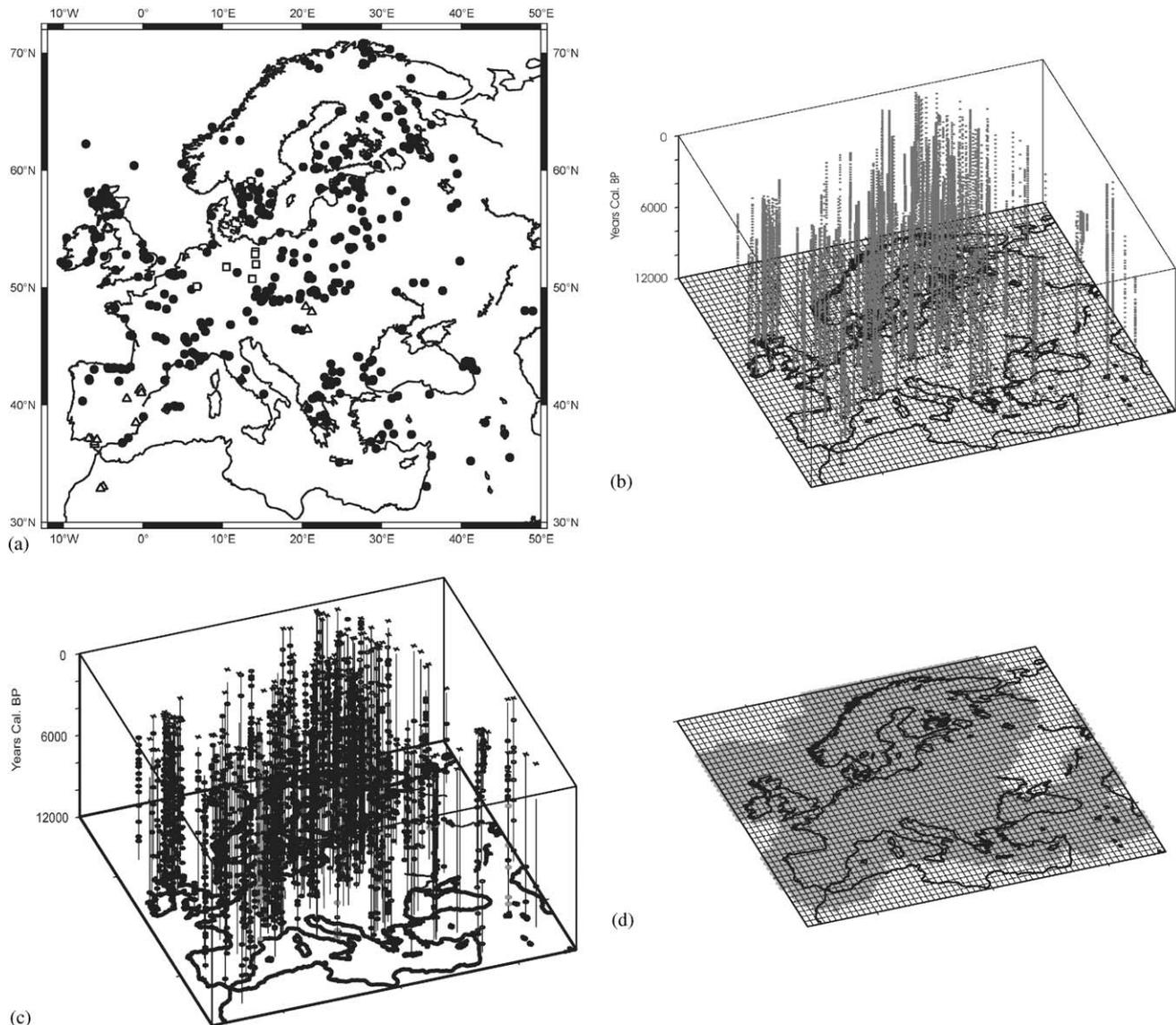
Fig. 1. (a) The distribution of pollen sites used in the study. The data for these sites was obtained from the European Pollen Database (●), the PANGAEA database (□), and individual contributors (Δ). (b) The distribution in time and two-dimensional space of the pollen samples used in the study. (c) The age-depth control points are shown for each core. These include radiocarbon dates (●), together with other absolute dates, such as those based on Laminations, Uranium series, Argon/Argon and Tephra (◖), as well as the core top where this was contemporary (×). In some cases these have been supplemented by relative dates based on stratigraphic correlation (○). (d) Following pollen-climate calibration, the data was then projected onto a 1° grid at a 100-year time step using a four-dimensional interpolation method. A series of statistical tests were then used to define a sub-set of the gridded data (grey) based on a minimum spatial and temporal sample density. This subset was used in all subsequent analysis.

and modern analogues rather than relying on a limited range of indicator taxa. We therefore substitute a modern analogue technique for the neural network technique used by Peyron et al. (1998) in the first study to reconstruct climate from PFT scores.

The use of PFT scores increases the number of pollen taxa that can be used within the analysis, whilst at the same time reducing the need for taxa-specific modern analogues. As a result, a much wider range of taxa can be included, including those that do not occur in the modern calibration dataset. For instance, *Buxus* was

once an important forest shrub in the Western Mediterranean (Yll et al., 1997), but is rarely found today, and consequently is not included in our training set. Using the PFT approach we are able to find a modern analogue for *Buxus* with other cool-temperate broad-leaved evergreens such as *Hedera* and *Ilex* that occur more widely today. The prevailing assumption is that individual taxa that share the same PFT group also share the same bioclimatic space (Peyron et al., 1998), which is in turn different from other taxa within other PFT groups. By grouping taxa in this way, the method is

Table 1
Observed and pollen-inferred modern climate values based on leave-one-out analysis

Climate variable	Correlation (r^2)	RMSE
MTCO	0.83	2.58
MTWA	0.75	2.25
TANN	0.80	2.35

MTCO; mean temperature of the coldest month, MTWA; mean temperature of the warmest month, TANN; mean annual temperature.

also less sensitive to changes in taxa abundance within the same PFT group, which may reflect non-climatic ecological or anthropogenic factors. This therefore reduces the influence of these factors may have on the climatic reconstruction.

Pollen taxa were converted into PFT values using the Peyron et al. (1998) PFT classification scheme for Europe, which defines 21 PFT groups using 93 pollen taxa. Evaluation of the method based on leave-one-out cross-validation using the surface sample dataset is presented in Table 1. This involves systematically removing each pollen sample from the training set and then predicting (reconstructing) its observed climate using the remaining pollen samples ($n-1$). The results are reported as the root mean square error (RMSE) and the coefficient of determination (r^2) (Birks, 1995). The results show that reconstructed values closely match the observed values, with a slightly better performance for the mean temperature of the coldest month (MTCO) than annual temperature (TANN), with both performing better than the mean temperature of the warmest month (MTWA). Following the assignment of a palaeoclimate and age to each fossil pollen sample, all the samples were then combined into a single dataset together with location information (latitude, longitude and altitude). The distribution of these samples in time and two-dimensional horizontal space is shown in Fig. 1b, with each core represented by a string of samples leading back in time.

3.2. Gridding and four-dimensional interpolation

Gridding data allows the changing spatial distribution of samples over time to be stabilized so that direct comparisons can be made more easily at the same locations between different time periods. It also allows area averages to be calculated which more accurately reflect the changing conditions across an area than simple sample averages that may contain bias by virtue of their distribution. This distribution is 3-D, with sites/samples located at different altitudes as well as the horizontal 2-D distribution typically shown on maps. Each grid point is also located in 3-D space, with grid-point altitude calculated from a digital elevation model (DEM) sampled at the same spatial resolution. Vertical

temperature gradients are often considerably steeper than horizontal climate gradients, and the correct representation of topography is important in order to arrive at an appropriate estimation of an area-average value. Projection on to a 3-D grid surface can also take into account changes in vertical temperature gradients (lapse-rates) through time. These are effectively ignored in simplistic 2-D maps that assume static vertical gradients through the use of anomalies (modern observation−fossil observation) to account for altitudinal differences.

Projection of data onto a grid requires the interpolation of data from the point of observation to the grid point position. This process becomes less reliable as the density of the observations decreases and interpolation distance increases. In order to constrain further the interpolation process in the estimation of grid point values and missing observations, Lou et al. (1998) have proposed that information from observations in space can be supplemented by observations in time. The authors found that this temporal–spatial approach to interpolation provided a more accurate basis for estimating values in the construction of instrumental time-series datasets. Palaeoclimate datasets also represent similar observational time series, although, as we have already established, the timing of the observation in many archives and proxies is more uncertain. This uncertainty, together with that involved in the calibration process, represents an additional source of noise in the estimation process. We believe however that detecting the underlying signal behind this noise can be greatly aided by applying this spatial–temporal approach within a large data network. This is because climate has a strong temporal, as well as spatial component. This is revealed in the many high- and low-frequency patterns identified on decadal–centenial (NAO, ENSO), centennial–millennial (Bond and Dansgaard-Oeschger cycles) and millennial + (Milankovich cycles) time scales (Wilson et al., 2000; Bond et al., 2001; Jones et al., 2001). These patterns have wide regional and even global footprints, which means their effects will also be felt over a wide spatial area, and therefore reflected in a large number of observations.

We have compiled a palaeoclimate dataset from hundreds of sites and thousands of samples within the relatively small geographical area of Europe. By treating this data as a single observational record in 4-D, we believe we can improve the signal-to-noise ratio to reveal the underlying pattern of climate change. This is based on the assumption that while erroneous data will inevitably occur within the dataset, this will be randomly distributed within a predominantly reliable set of observations. The interpolation process acts to isolate this erroneous data in two ways, first by being guided by the greater majority of the data, and secondly by reinforcing the non-random spatial–temporal patterns
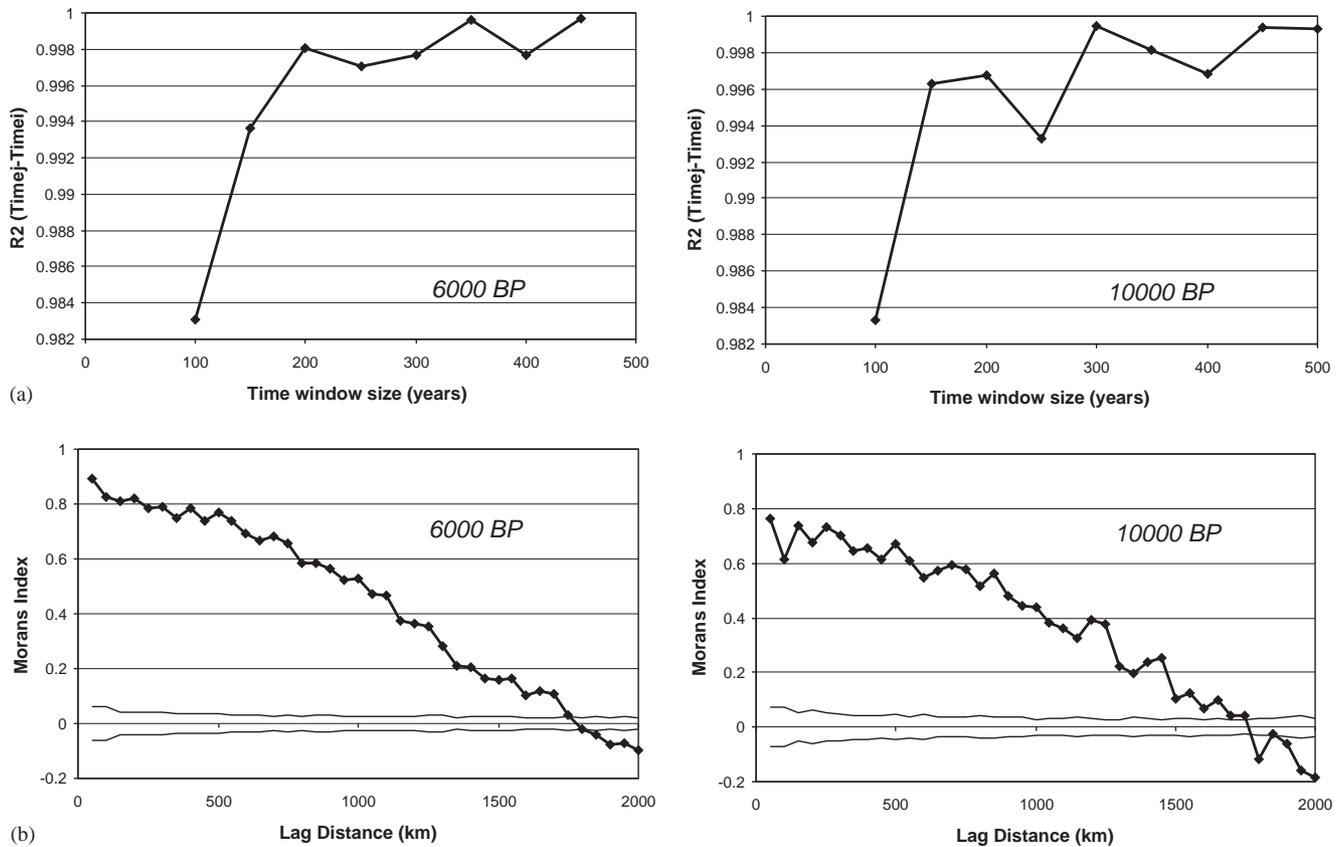
Fig. 2. (a) Comparison of estimations for MTCO for the target time based on an increasing time window (50-year step). Value on *y*-axis is R2 of current time window (Time*j*) compared with previous time window (Time*i*). Left: 6000 BP; right: 10,000 BP. (b) Moran's Index calculated for MTCO over a series of distance lags (in kilometres). Bold line shows calculated index value at each lag; thin lines show limits of expected values calculated for random permutations of data (99 iterations). Left: 4000 BP; right: 8000 BP.

within the data. Assimilation through interpolation therefore acts to focus the reconstruction within a haze of uncertainty.

Interpolation of the data was carried out using a 4-D smoothing spline (Nychka et al., 2000), similar to the approach used by Lou et al. (1998). This method uses generalized cross-validation to determine the optimal fit of the spline volume to the data. Once the spline model has been built, climatic values were estimated at the grid points of the study area. The output grid was one degree by one degree with a temporal resolution of 100 years. Altitudes were taken as averages from a 5 min DEM (TerrainBase, Row et al., 1995). The temporal resolution almost certainly exceeds the inherent resolution of the data, and should not be taken to imply that climate events can be resolved within a 100-year time frame. Rather, it can be compared to regular plotting of a variable running mean whose time frame generally exceeds the time interval between the plotting points. In this case, the chosen interval may or may not reveal statistically significant events when the time frame of the running mean approaches that of the plotting interval. In the case of the present study, we do

not attempt to interpret sub-millennial scale events shown in the data.

Due to computational limitations, we were unable to produce a spline model for the entire dataset. Interpolation was instead carried out for the study area at each temporal grid point (each 100-year time step). Data were included within ±300 years of the time period of interest giving a series of overlapping datasets, each containing 600 years of samples. The 300-year limits were chosen by testing the effects of increasing the size of the time window on the estimated values across the study area for a number of different periods. Starting with data at ±50 years, the time window was increased in 50-year steps until no further changes were seen in the resulting estimations. This limit was found at between 250 and 300 years for all time periods, indicating that the inclusion of data beyond 300 years either side of the target time has little significant influence on the result (Fig. 2a). A data window of ±300 years was therefore used for each time step, representing a de facto limit of data independence. This means that any two reconstructions at time steps 600 years apart have been based on entirely independent sets of data.

As the quality of the interpolation will vary across the study area, depending on the distance (in both space and time) from the samples, a subset of the interpolated grid points was selected for subsequent analysis. The selection was made by including only those geographical grid points that were consistently within a pre-defined distance of at least one sample over the study period of 12,000 years. The spatial autocorrelation of samples was studied in several periods to define a reliable spatial limit. Samples were shown to be positively correlated to over 1500 km (Fig. 2b), but we chose to apply a more conservative limit of 500 km. This limit was shown to have significant positive correlation by Moran's Index ($p < 0.01$) (Moran, 1950; Cliff and Ord, 1981). The 500 km limit was combined with the previously established temporal limits of ± 300 years to form a minimum spatial–temporal sample density. Using a GIS, we then isolated a core area (Fig. 1d) where this minimum sample density was maintained throughout the study period.

It has already been mentioned that the technique acts to isolate the influence of erroneous data. This will of course only apply when this data represents a minority of observations within the dataset, a factor influenced by the quantity of data. To ensure that the reconstructed climatic signals were based on a large number of sites, we assimilated the gridded data into six large-scale regional records. Area-average time series were then calculated for these records, each based on a large number of sites.

3.3. Isostatic readjustment

The assignment of altitude to the grid network has been based on modern topography with no correction through time for isostatic uplift. The effect of uplift is to make temperature reconstructions appear warmer than would be expected during the early Holocene when the land surface was lower. This could be locally significant in our NE region where post-glacial uplift has been calculated at over 300 m in some areas around the Gulf of Bothnia in the Baltic Sea. Attempts at correcting for this discrepancy have been made in some studies (e.g. Rosen et al., 2001), although they are based on the assumption that lapse rates have remained constant at around $-0.6°C/100$ m. These assumptions however are unlikely to hold true in the lower part of the atmosphere where lapse rates vary seasonally and spatially due to interaction with the ground surface. An analysis of lapse rates using NCEP/NCAR re-analysis data reveals the current mean annual lapse rate for the NE region in the upper atmosphere (850–700 mbar) is $-0.5°C/100$ m. However, this value falls to $-0.3/100$ m in the lower atmosphere (Surface to 850 mb height, or approximately 0–1800 m asl), ranging from $0.0°C/100$ m in January to $-0.5°C/100$ m in July. These values fluctuated by as much

as $0.3°C$ in January and $0.1°C$ in July between 1958 and 98. Other studies have also suggested changes in lapse rates on Holocene time-scales in temperate (Huntley and Prentice, 1988), and tropical regions (Peyron et al., 2000). A large amount of uncertainty therefore remains over this problem, although the system of 3-D spatial interpolation corrects for lapse rate change, and the area most affected by isostatic readjustment remains small with few core sites. The impact of isostatic changes on the reconstruction is therefore probably not significant at the regional scale.

4. Results and discussion

All results are shown as anomalies compared to the 60 BP (1890) reconstruction. The modern -40 BP (1990) reconstruction was not used as the baseline because this time step was not based on a balance of samples both forward and back in time. Reconstructions are represented by six regional time series (Figs. 3 and 4), together with summary reconstructions for the whole European area (Fig. 5). In comparing these results with data from individual sites or smaller local regions it is important to remember that they represent area averages over large regions within which large local differences can occur. Similarly, the choice of summary regions has been relatively arbitrary, while the climate changes shown can be expected to form a continuum between regions such that selection of a different geographical region will produce a subtlety different pattern of change based on the same underlying pattern.

4.1. Northern Europe

Reconstructed summer MTWA anomalies across Northern Europe during the early Holocene show values comparable with modern temperatures. These then rise to a clear maximum around 6000 BP, with the onset of this rise delayed to around 9000 BP in the east. At their peak, MTWA anomalies reach $+1.5°C$ in the NW sector and $+1.0°C$ in the NE sector, before declining through the remainder of the Holocene. Winter MTCO anomalies are much greater than late Holocene values at the start of the Holocene, ranging from $-9.0°C$ in the NW region, to $-2.0°C$ in the NE. After a rapid rise at 11,500 BP to around $-5.0°C$, temperatures in the NW region then show a steady rise to present day values. In the NE, temperatures rise more quickly to values at, or slightly above, late Holocene values around 7000 BP. Overall annual TANN anomalies are lower in the NW at the onset of the Holocene than the NE region, reflecting the lower winter temperatures. Annual temperatures in both regions then rise until 6500 BP, before stabilizing in
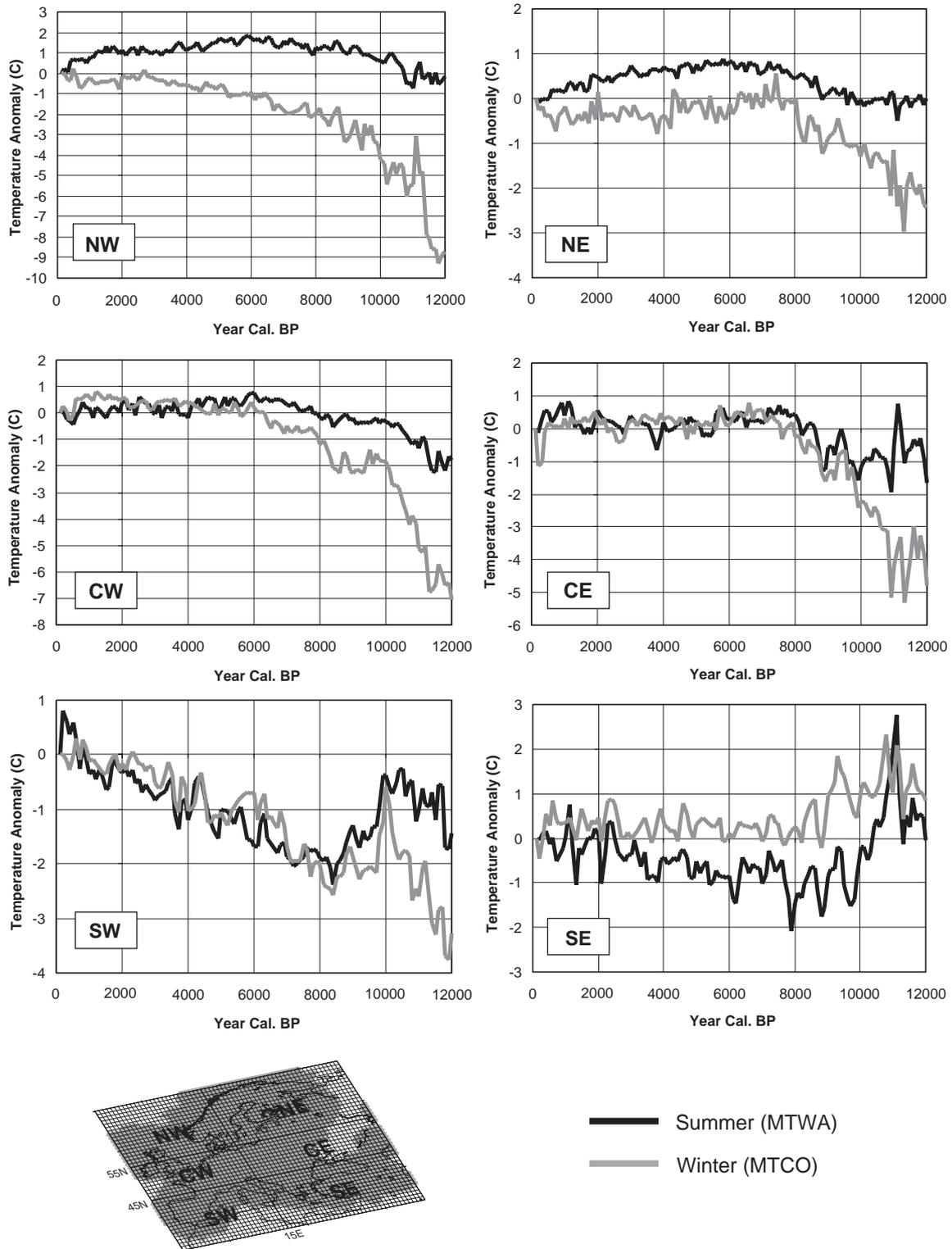
Fig. 3. Reconstructed area-average summer (MTWA) and winter (MTCO) temperature anomalies for six regions in Europe during the Holocene.

the NW, and undergoing a late Holocene decline in the NE.

A large number of studies have attempted to reconstruct Holocene temperature changes across

northern Europe from a wide variety of archives and proxies. Increasingly, these have provided quantitative estimates at the site scale, although attempts at systematic regional scale analysis directly comparable
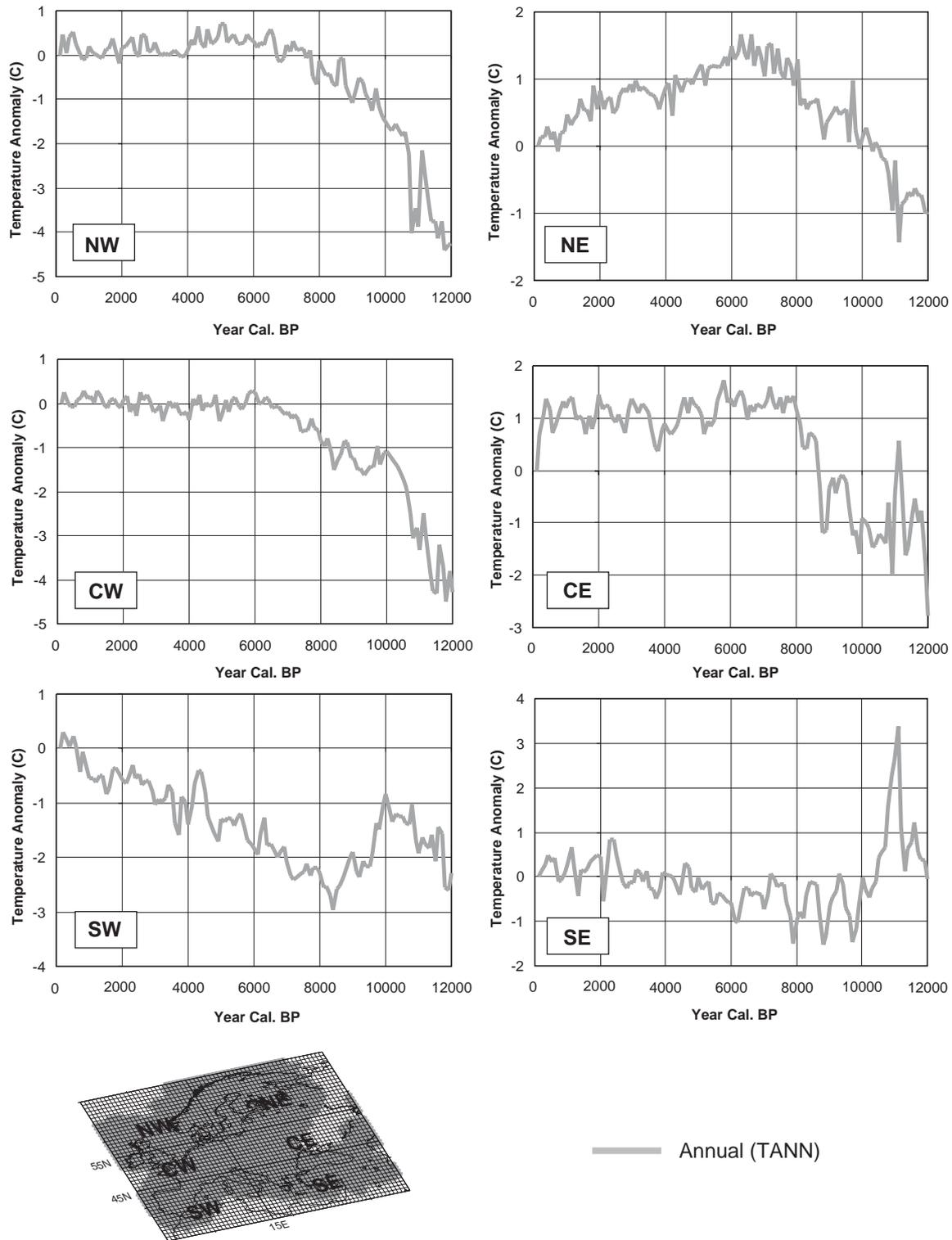
Fig. 4. Reconstructed area-average mean annual (TANN) temperature anomalies for six regions in Europe during the Holocene.

with our own estimates remain few. Despite this, comparison of existing site-specific reconstructions across Northern Europe indicate close agreement with our results.

Early Holocene summer temperatures similar to the present day were also reconstructed in Northern Scandinavia by Seppä and Birks (2001) using pollen and Rosén et al. (2001) using a range of proxies,
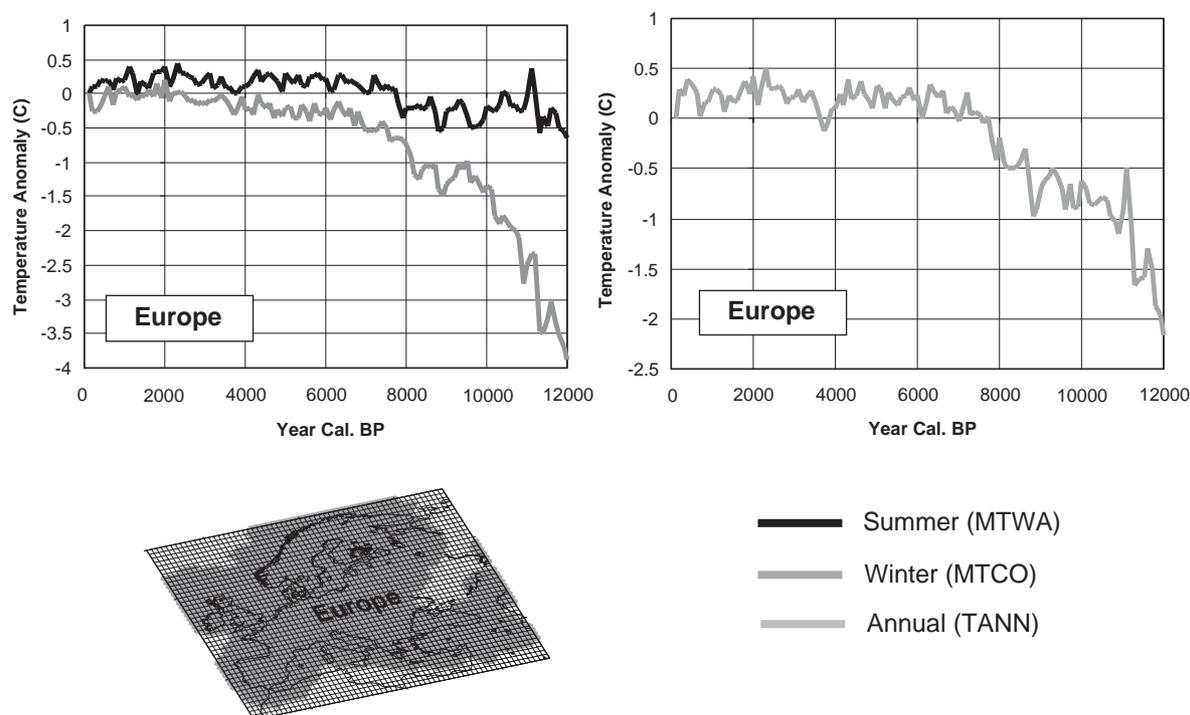
Fig. 5. Reconstructed area-average summer (MTWA) and winter (MTCO) temperature anomalies (a), and annual temperature (TANN) anomaly (b) for Europe during the Holocene.

including pollen, chironomids, diatoms and NIR. In another quantitative multi-proxy study in Western Norway, Birks and Ammann (2000) found summer temperatures at the start of the Holocene increased quickly to values close to modern levels, and warming continued into the early Holocene. Other studies based on macrofossil reconstructions of past tree-lines have also noted that the early Holocene tree-line was close to the present day in the Scandes mountains (Dahl and Nesjke, 1996). These and other studies also indicate that the early Holocene warming was gradual (Karlén, 1998; Lauritzen and Lundberg, 1999; Seppä and Birks, 2001).

Evidence for a mid-Holocene thermal maximum in Scandinavia is considerable, and based on a wide range of proxies. Tree-lines reached their maximum altitude up to 300 m higher than today (Eronen and Zetterberg, 1996; Barnekow and Sandgren, 2001) and glaciers were much reduced or absent (Karlén, 1988; Seierstad et al., 2002). Quantitative reconstructions indicate that temperatures were up to 2.0°C higher than today (Barnekow, 2000; Barnett et al., 2001; Seppä and Birks, 2001, 2002; Rosén et al., 2001). These mostly refer to summer temperatures, although Kullman (1995) notes that the success of pine in the early Holocene in the Scandes mountains would not have been compatible with colder (and drier) than normal winters even if the summers were warmer. Higher temperatures may also have increased evaporation, contributing to the decline in

mid-Holocene lake levels observed between 8000 and 5800 BP by Hyvärinen and Alhonen (1994).

Our results suggest the summer thermal maximum occurred across a wide area of Northern Europe at around 6000 BP. Evidence from other studies indicate a range of dates for the timing of the mid-Holocene thermal maximum, although many of these fall between 6000 and 7000 BP. These include dates of between 7900 and 6700 BP from pollen data (Seppä and Birks, 2001), 6200 BP from chironomids (Korhola et al., 2000) and maximum tree-line altitudes at 6300 BP (Barnekow, 2000) and between 6300 and 4500 BP (Barnekow and Sandgren 2001; Seppä et al., 2002). Land ice cover was also at a minimum at 6200 BP (Nesje et al., 2001), whilst glaciers were mainly absent from a catchment in Western Norway between 9800 and 6700 BP (Seierstad et al., 2002), and between 7300 and 6100 BP at least the northern part of the Jostedalsbreen ice cap melted away (Nesje et al., 2000).

Discrepancies in the timing of the thermal maximum between studies may be related to local climatic effects, or edaphic factors in the case of vegetation proxies. The Scandes mountains form one of the steepest climatic barriers in Europe, and sites either side of them may be expected to show contrasting responses. Seppä and Birks (2002) showed that the mid-Holocene maximum may vary even within a relatively short distance using the same reconstruction methods and calibration dataset. For other proxies sensitive to different climatic

forcing, the contrasting pattern of MTCO and TANN also suggests that different seasonal sensitivities may account for inter-proxy discrepancies. For instance, the timing of the maximum for TANN is 1000 years earlier (and the anomaly is greater) than MTWA in the NE sector as a result of warmer spring and/or autumn temperatures, possibly as a result of more prolonged ice-free conditions in the Barents Sea (Duplessy et al., 2001). Multi-proxy studies from the same site location indicate differences in the reconstructed temperature record between proxies (Rosén et al., 2001). Korhloa et al. (2002) also note that the current distribution of macrofossil evidence used to infer tree-line change may be as much a result of favourable preservation as climate.

Following the mid-Holocene maximum, almost all studies then report a late-Holocene cooling as neoglacial conditions became established (Rosén et al., 2001; Seppä and Birks, 2001, 2002; Korhola et al., 2002). Glaciers expanded (Karlén, 1988; Nesje et al., 2001; Seierstad et al., 2002) and tree-lines retreated (Dahl and Nesje, 1996; Barnekow, 2000; Barnett et al., 2001). This pattern of late-Holocene cooling is repeated in our own data, more especially in summer temperatures, while winter temperatures continued to rise in the NW sector. Temperatures do not however fall below early Holocene values, and our data does not support the idea of Bigler et al. (2002) that the last four millennia were the coldest of the entire Holocene. The largest cooling is in MTWA in the NW sector and TANN in the NE sector with mid-Holocene anomalies of almost $+1.5°C$. High mid-Holocene TANN values in the NE region were also reconstructed by Shemesh et al. (2001) on the basis of the $\delta^{18}O$ of biogenic silica from Swedish Lapland. Values however were much higher, and the subsequent neoglacial cooling estimated at between 2.5 and 4.0°C. In the NW sector, TANN was balanced between cooling summer temperatures and warming winter temperatures. This pattern of relative stability in Holocene TANN is supported by another $\delta^{18}O$ record from a speleothem in coastal Norway which shows little long-term trend in TANN after reaching present-day values around 9000 BP (Lauritzen and Lundberg, 1999).

4.2. Central Europe

Early Holocene summer MTWA anomalies were lower across Central Europe than Northern Europe, particularly in the CW sector where anomalies were up to $-2.0°C$ at the onset of the Holocene. Winter anomalies were also colder in the CE region than NE region, although temperature anomalies in the west were approximately the same following the rapid warming at the end of the Younger Dryas in the NW region. Both summer and winter anomalies in the CW region then follow a similar pattern to the NW region, with a mid-Holocene summer maximum around 6000 BP, while winter temperatures continue to rise, with the overall result that annual temperatures stabilize as summers cool after 6000 BP. The CE region also shows many similarities with the NE region, with delayed summer warming, but also a much less well-defined mid-Holocene maximum. This reflects a much lower overall variation in mid–late-Holocene temperatures in the Central European area, with no real trend in seasonal or annual temperatures in the CE region after 8000 BP.

In comparing our results with other palaeoclimate records from the Central Europe region, it is clear that far fewer records show the large and coherent Holocene warming and cooling trends that characterize Northern Europe. After an initial period of early Holocene warming, our results show temperature fluctuations generally within 1.0°C of modern values, in agreement with Alpine reconstructions (Haas et al., 1998). The small magnitude of change and lack of clear trend is probably why many paleoclimate records from the region show a Holocene climate characterized by short-term periodic events rather than consistent long-term trends (e.g. Magny, 1993).

We reconstruct early Holocene summer temperature anomalies that were cooler across Central Europe than Northern Europe, whilst MTWA anomalies were still less than winter MTCO values. Cooler early Holocene temperatures and colder winter anomalies were also found by Atkinson et al. (1987) who looked at Coleoptra evidence from a number of sites in Britain. In this regional study, MTWA anomalies were consistently less than MTCO anomalies, whilst overall mean anomaly values were around 2.0°C cooler than our reconstruction for the CW sector. Some of this discrepancy may be accounted for by the fact that a number of the sites considered in this study lie close to the NW sector, which experienced greater winter anomalies during this time.

By 8000 BP, temperatures in all seasons had recovered across Central Europe to values within 1.0°C of modern values. In the east, temperatures fluctuated within these limits for the remainder of the Holocene with no clear trends. This agrees with a wealth of evidence from Alpine regions indicating periodic glacier advance and retreat during the Holocene (Hormes et al., 2001). Quantitative estimates based on plant macrofossil and pollen evidence by Haas et al. (1998) also suggest summer temperature varied within 0.7–0.9°C above present.

Our results show that the mid-Holocene thermal maximum at 6000 BP is more clearly defined in the west than the east, where the warming occurred earlier and throughout all seasons. In Austria, the Pasterze Glacier was limited in extent during the early Holocene, and was smaller than present for an extended period between 8100 and 6900 BP (Nicolussi and Patzelt, 2000). Further

west, evidence for a later and more pronounced mid-Holocene warming is supported by Zoller et al. (1998) and Haas et al. (1998), who found tree lines were highest in Switzerland around 6000 BP. Less well-dated studies have also identified maximum timberline altitudes in the Alps between 9000 and 4700 BP (Tinner et al., 1996) and 8700 and 5000 BP (Wick and Tinner, 1997). In Italy's Aosta Valley, Burga (1991) identified the period 8300–6000 BP to be the warmest period during the Holocene, with maximum warmth between 6700 and 6000 BP when tree-lines were located 100–200 m above present levels. From this timberline change, Burga (1991) estimated summer temperatures were 1.5–3.0°C higher than present during this period. This is higher than our own estimates, which are more in agreement with the Haas et al. (1998) study, which is also based on a wider range of sites.

Following the mid-Holocene maximum, summer temperatures declined in the west, although winter temperatures continued to increase. In the Alps, timberlines retreated, although this has also been partly attributed to human action (Tinner et al., 1996). Evidence of cooler conditions is supported by Barber et al. (1994) who noted changes in peat macrofossils indicating wetter bog surfaces in NW Europe after 4500 BP, while Mauquoy and Barber (1999) also noted increasing surface wetness in British bogs in the last millennium. Circumstantial evidence for cooling also comes from the recent discovery in the Alps of a superbly preserved prehistoric man melting from ice high on the Austrian–Italian border. Radiocarbon dating of the body suggests that it was buried between 5000 and 5300 BP, immediately preceding neoglaciation (Baroni and Orombelli, 1996).

Further west in the CW region, a cool early Holocene, warm mid-Holocene and late-Holocene neoglacial is also supported by the speleothem oxygen isotope record from SW Ireland. McDermott et al. (1999) interpreted low $\delta^{18}O$ conditions in the early Holocene as reflecting cooler conditions, with $\delta^{18}O$ increasing between 9000 and 6000 BP as warmer conditions became established, followed by another cooling trend between 7800 and 3500 BP. However, they also suggested increasing $\delta^{18}O$ since 3500 BP could possibly indicate a return to warmer conditions. A second higher resolution study (McDermott et al., 2001) revealed a more complex record, but overall reflecting the same larger scale changes.

4.3. Southern Europe

The pattern of Holocene temperature change reconstructed for Southern Europe generally follows a very different pattern from the regions to the north. Early Holocene summer MTWA and winter MTCO anomalies were actually positive over the SE region, and only slightly negative in the SW in summer. Winter

temperature anomalies were −3.0°C at the Younger Dryas–Holocene transition over the SW region, but even here they had recovered close to modern levels by 10,000 BP. Temperatures then fell around 1.5°C across the whole region and at all seasons up to 8000 BP, before an almost linear increase up to modern values for all except winter temperatures in the SE. These did not fall below present day values at 8000 BP, and have generally maintained themselves at the same level through to the present day.

Comparison with existing reconstructions is difficult for Southern Europe because there have been relatively few quantitative climate reconstructions, and even fewer that provide estimates of temperature variables. Terral and Mengüal (1999) used the anatomy of olive charcoal to estimate temperatures during the early and mid-Holocene in southeast Spain and southern France. They reconstructed annual temperatures between 1.5°C (France) and 3.5°C (Spain) lower than present, in agreement with our own reconstructions for the Western Mediterranean. Similarly, on the basis of $\delta^{18}O$ analysis of a speleothem in Southern France, McDermott et al. (1999) suggested the climate of Southern France was cooler than present during the early to mid-Holocene. Interestingly, the authors noted that this represented an opposing trend to the speleothem record from SW Ireland, a comparison also supported by our own study.

Other palaeoclimate reconstructions suggest changes in water balance that could have been brought about by changes in temperature and/or precipitation. Cool temperatures and/or higher precipitation in the early to mid-Holocene have been proposed by Harrison and Digerfeldt (1991) to explain high lake levels throughout the Mediterranean at this time. They also note that Holocene aridity was established more abruptly in the west than the east where lake levels declined more slowly. This latter finding is compatible with our own that temperatures (and hence evaporation) during the important winter recharge period increased along with summer temperatures in the west, but remained relatively stable in the east. Other studies also support high lake levels during the early to mid-Holocene in locations in both the east (Landmann and Reimer, 1996; Roberts et al., 2001) and west (Roca and Juliá, 1997; Giralt et al., 1999; Reed et al., 2001).

Wetter early to mid-Holocene conditions have also been suggested from isotopic analysis of fossil charcoal in southern France (Vernet et al., 1996), as well as speleothems in Israel (Bar-Matthews et al., 1997). Further evidence for anomalous cool or wet conditions comes from the presence of an early Holocene sapropel in the Mediterranean marine record centred around 8000 BP and spanning between ca 10200 and 6400 BP (Mercone et al., 2000). The timing of this event coincides with a reduction in summer MTWA and annual TANN

temperatures in both the SW and SE regions in our own study. SST reconstructions for this time period remain ambiguous however, with some authors suggesting cooler conditions (Kallel et al., 1997; Geraga et al., 2000), and others warmer conditions (Emeis et al., 2000; Marchal et al., 2002). In contrast to our own study, the inferred prevailing climate in a number of marine-based studies has also invariably been interpreted as warm and wet (Myers and Rohling, 2000; Rohling and De Rijk, 1999; Ariztegui et al., 2000).

4.4. All of Europe

Assimilating the six regional records gives the total mean change in area-average temperatures across Europe (Fig. 5). This reveals the seasonal and annual thermal budget for the continent, allowing comparison with global insolation and ice cover changes, which represent the dominant controls on climate on Holocene time-scales. The results indicate no long-term trend through the Holocene in summer MTWA anomalies, with only a step-wise increase in temperature around 7800 BP. This contrasts with winter MTCO that shows steadily attenuating anomaly values throughout the Holocene as temperatures rose to present day levels. Overall annual temperature change shows that these seasonal changes occurred within a well-constrained annual thermal budget, which grew linearly from the onset of the Holocene up to 7500 BP. After this point, annual temperatures remained steady for the remainder of the Holocene.

This reconstruction does not show a mid-Holocene thermal optimum, as has been suggested by many authors (Houghton et al., 1990). This is in agreement with previous pollen-based studies for this period, which demonstrated that summer warming was confined to Northern Europe whilst Southern Europe cooled (Cheddadi et al., 1997). Here we show however that, not only was high latitude mid-Holocene warming numerically balanced by low latitude cooling, this balance was maintained throughout the Holocene. We can therefore show no summer temperature response at the European scale to increased summer insolation (Kutzbach and Webb III, 1993).

The stability of summer temperatures indicates that the principal control on Holocene temperatures has come from changes in winter MTCO temperatures. These show an increase that superficially appears in line with increasing winter insolation, however, annual TANN temperatures reveal that this can be more clearly linked to the decline in residual LGM ice cover that occurred up to 7500 BP (Kutzbach and Webb III, 1993). This melting ice also led to rising global sea levels, which have since stabilized. There is no evidence of a late-Holocene decline in sea levels that would be expected with widespread neoglaciation following a mid-Holo-

cene thermal maximum (Broecker, 1998). Our results are therefore in agreement with this model of Holocene climate change.

5. Conclusions

We have shown that by assimilating many thousands of individual pollen-based proxy-climate observations through four-dimensions using a GIS, it is possible to provide an entirely new quantitative and dynamic perspective on Holocene climate change. The internal consistency of the results and their agreement with other proxy records suggests that the influence of local climatic and non-climatic factors on the reconstruction method has been limited. This can be attributed to both the large continental scale of the analysis, and the use of pollen PFT scores in the calibration process. This has revealed coherent climatic trends even in Southern Europe and the Mediterranean, despite a fragmented and anthropogenically disturbed record. Summer and winter temperatures show a high degree of independence, indicating that the reconstruction is not being restricted by co-variance amongst climate variables. Trends established in the early to mid-Holocene appear consistent with those in the later-Holocene, suggesting that unique vegetation associations found in the early Holocene (Huntley, 1988) have found valid modern analogues.

The method shows the importance of maintaining a balance between the need for careful individual site interpretation, and a similar need for a large-scale perspective. Assimilation of sites within a single database linked through space and time provides the basis for mutually supportive holistic analysis that is greater than the sum of the individual sites. This approach will be greatly improved in future through the application of probabilistic interpolation techniques based on full error accounting of the age-depth and pollen-climate calibration. This in turn will provide a basis for improving the temporal and spatial resolution of the reconstructions, and allow the statistical assessment of their significance.

We have provided in this analysis the first quantitative assessment of continuously changing seasonal and annual surface temperatures across Europe during the Holocene. This analysis has produced a number of important findings:

1. Significant regional and seasonal variations in temperature patterns have nevertheless occurred within a remarkably balanced total energy budget. This budget has remained stable following the final disappearance of residual LGM ice around 7800 BP. There has been no net annual response to seasonal changes in insolation, and no apparent late Holocene neoglacial cooling at the European scale.

2. The traditional mid-Holocene thermal maximum is shown to be confined to Northern Europe, and more especially to the summer months. This insolation driven warming was balanced by a mid-Holocene thermal minimum over Southern Europe counter to the expected insolation response. The cooling is also counter to some marine-based interpretations of mid-Holocene climate in the Mediterranean.

3. Summer temperature changes have been smaller than winter temperature changes in all regions apart from the SE. Changes in winter temperatures have therefore been a more significant control on the total energy budget than summer temperatures. The greatest changes in winter temperatures have been in the maritime west of Europe where warming has occurred almost continuously throughout the Holocene.

4. From the mid-Holocene onwards, temperatures in Central Europe have only shown small-scale changes without the large-scale warming/cooling trends that characterise the areas to the north and south. This stability probably accounts for the preponderance of studies from this area that argue for a Holocene climate of short-term fluctuations.

5. Southern Europe and the Mediterranean have undergone an almost linear warming from around 8000 BP. This warming predates the onset of any major human impact and continues at the same rate through the anthropogenically important late-Holocene. This suggests not only a predominantly natural origin for the Mediterranean climate, but also that the pollen-climate calibration method has remained independent of human impact on the vegetation.

6. Summer MTWA, winter MTCO and annual TANN temperatures have undergone very different trends both within and between regions. Attempts to over-generalize on the basis of seasonally restricted proxies or geographically restricted archives should be treated with caution. Only through seasonally and spatially adjusted area-average calculations can the effect of seasonal and local scale variations in energy balances be correctly assessed at annual and continental scales.

Appendix

Data sources: EPD European Pollen Database, available from: http://www.ngdc.noaa.gov/paleo/epd.html

PANGAEA Network for Geological and Environmental Data, available from: http://www.pangaea.de/

NCEP/NCAR Monthly reanalysis data, available from: http://www.cdc.noaa.gov/cdc/reanalysis/reanalysis.shtml

References

Ariztegui, D., Asioli, A., Lowe, J.J., Trincardi, F., Vigliotti, L., Tamburini, F., Chondrogianni, C., Accorsi, C.A., Mazzanti, M.B., Mercuri, A.M., Van der Kaars, S., McKenzie, J.A., Oldfield, F., 2000. Palaeoclimate and the formation of sapropel S1: inferences from Late Quaternary lacustrine and marine sequences in the central Mediterranean region. Palaeogeography, Palaeoclimatology, Palaeoecology 158 (3–4), 215–240.

Atkinson, T.C., Briffa, K.R., Coope, G.R., 1987. Seasonal temperatures in Britain during the last 22,000 years reconstructed using beetle remains. Nature 325, 587–592.

Barber, K.E., Chambers, F.M., Maddy, D., Stoneman, R., Brew, J.S., 1994. A sensitive high resolution record of late Holocene climatic change from a raised bog in northern England. The Holocene 4, 198–205.

Bar Matthews, M., Ayalon, A., Kaufman, A., 1997. Late Quaternary paleoclimate in the eastern Mediterranean region from stable isotope analysis of speleothems at Soreq Cave, Israel. Quaternary Research 47, 155–168.

Barnekow, L., 2000. Holocene regional and local vegetation history and lake-level changes in the Tornetrask area, northern Sweden. Journal of Paleolimnology 23 (4), 399–420.

Barnekow, L., Sandgren, P., 2001. Palaeoclimate and tree-line changes during the Holocene based on pollen and plant macrofossil records from six lakes at different altitudes in northern Sweden. Review of Palaeobotany and Palynology 117, 109–118.

Barnett, C., Dumayne-Peaty, L., Matthews, J.A., 2001. Holocene climatic change and tree-line response in Leirdalen, central Jotunheimen, south central Norway. Review of Palaeobotany and Palynology 117, 119–137.

Baroni, C., Orombelli, G., 1996. The Alpine 'Iceman' and Holocene climatic change. Quaternary Research 46, 78–83.

Bigler, C., Larocque, I., Peglar, S.M., Birks, H.J.B., Hall, R.I., 2002. Quantitative multiproxy assessment of long-term patterns of Holocene environmental change from a small lake near Abisko, northern Sweden. The Holocene 12 (4), 481–496.

Birks, H.J.B., 1995. Quantitative palaeoenvironmental reconstructions. In: Maddy, D., Brew, J.S. (Eds.), Statistical modeling of Quaternary Science Data, Technical Guide, Vol. 5. Quaternary Research Association, Cambridge, pp. 161–254.

Birks, H.H., Ammann, B., 2000. Two terrestrial records of rapid climatic change during the glacial-Holocene transition (14,000–9,000 calender years B.P) from Europe. Proceedings of the National Academy of Sciences 97 (4), 1390–1394.

Bond, G., Bernd, K., Beer, J., Muscheler, R., Evans, M.N., Showers, W., Hoffman, S., Lotti-Bond, R., Hajdas, I., Bonani, G., 2001. Persistent solar influence on North Atlantic climate during the Holocene. Science 294 (5549), 2130–2136.

Briffa, K.R., Osborn, T.J., Schweingruber, F.H., Harris, I.C., Jones, P.D., Shiyatov, S.G., Vaganov, E.A., 2001. Low-frequency temperature variations from a northern tree ring density network. Journal of Geophysical Research 106 (d3), 2929–2941.

Broecker, W.S., 1998. The end of the present interglacial: how and when? Quaternary Science Reviews 17, 689–694.

Bronk Ramsey, C., 2000. Radiocarbon calibration program available from: http://www.rlaha.ox.ac.uk/orau/06_01.htm.

Brovkin, V., Ganopolski, A., Claussen, M., Kubatzki, C., Petoukhov, V., 1999. Modelling climate response to historical land cover change. Global Ecology and Biogeography 8 (6), 509–517.

Burga, C.A., 1991. Vegetation history and paleoclimatology of the middle Holocene—pollen analysis of Alpine peat bog sediments, covered formerly by the Rutor Glacier, 2510 m Aosta Valley, Italy. Global Ecology and Biogeography Letters 1 (5), 143–150.

Cheddadi, R., Yu, G., Guiot, J., Harrison, S.P., Prentice, I.C., 1997. The climate of Europe 6000 years ago. Climate Dynamics 13, 1–9.

Cheddadi, R., Lamb, H.F., Guiot, J., van der Kaars, S., 1998. Holocene climatic change in Morocco: a quantitative reconstruction from pollen data. Climate Dynamics 14, 883–890.

Claussen, M., Mysak, L.A., Weaver, A.J., Crucifix, M., Fichefet, T., Loutre, M.F., Weber, S.L., Alcamo, J., Alexeev, V.A., Berger, A., Calov, R., Ganopolski, A., Goose, H., Lohmann, G., Lunkeit, F., Mokhov, I.I., 2002. Earth system models of intermediate complexity: closing the gap in the spectrum of climate system models. Climate Dynamics 18 (7), 579–586.

Cliff, A.D., Ord, J.K., 1981. Spatial Processes: Models and Applications. Pion, London, 266pp.

COHMAP members, 1988. Climatic changes of the last 18,000 years. Observations and model simulations. Science 241, 1043–1052.

Crucifix, M., Loutre, M.F., Tulkens, P., Fichefet, T., Berger, A., 2002. Climate evolution during the Holocene: a study with an Earth System model of intermediate complexity. Climate Dynamics 19 (1), 43–60.

Dahl, S.O., Nesje, A., 1996. A new approach to calculating Holocene winter precipitation by combining glacier equilibrium line altitudes and pine-tree limits: a case study from Hardangerjøkulen, central south Norway. The Holocene 6, 381–398.

Duplessy, J.C., Ivanova, E., Murdmaa, I., Paterne, M., Labeyrie, L., 2001. Holocene paleoceanography of the northern Barents Sea and variations of the northward heat transport by the Atlantic Ocean. Boreas 30 (1), 2–16.

Emeis, K.-C., Struck, U., Schulz, H.-M., Rosenberg, R., Bernasconi, S., Erlenkeuser, H., Sakamoto, T., Martinez-Ruiz, F., 2000. Temperature and salinity variations of Mediterranean Sea surface waters over the last 16,000 years from records of planktonic stable oxygen isotopes and alkenone unsaturation ratios. Palaeogeography, Palaeoclimatology, Palaeoecology 158, 259–280.

Eronen, M., Zetterberg, P., 1996. Climatic changes in Northern Europe since late glacial times, with special reference to dendroclimatological studies in northern Finnish Lapland. Geophysica 2, 35–60.

Ganopolski, A., Rahmstorf, S., 2001. Rapid changes of glacial climate simulated in a coupled climate model. Nature 409 (6817), 153–158.

Geraga, M., Tsaila-Monopolis, St., Ioakim, Chr., Papatheodorou, G., Ferentinos, G., 2000. Evaluation of palaeoenvironmental changes during the last 18,000 years in the Myrtoon Basin, SW Aegean Sea. Palaeogeography, Palaeoclimatology, Palaeoecology 156, 1–17.

Giralt, S., Burjachs, F., Roca, J.R., Juliá, R., 1999. Late Glacial to Early Holocene environmental adjustment in the Mediterranean semi-arid zone of the Salinas playa-lake Alicante, Spain. Journal of Paleolimnology 21, 449–460.

Guiot, J., 1990. Methodology of paleoclimate reconstruction from pollen in France. Palaeogeography, Palaeoclimatology, Palaeoecology 80, 49–69.

Guiot, J., Cheddadi, R., Prentice, I.C., Jolly, D., 1996. A method of biome and land surface mapping from pollen data: application to Europe 6000 years ago. Palaeoclimates 1, 311–324.

Haas, J.N., Rischoz, I., Tinner, W., Wick, L., 1998. Synchronous Holocene climatic oscillations recorded on the Swiss Plateau and at the timberline in the Alps. The Holocene 8 (3), 301–309.

Harrison, S.P., Digerfeldt, G., 1991. European lakes as palaeohydrological and palaeoclimatic indicators. Quaternary Science Reviews 12, 233–248.

Hormes, A., Müller, B.U., Schlüchter, C., 2001. The Alps with little ice: evidence for eight Holocene phases of reduced glacier extent in the Central Swiss Alps. The Holocene 11 (3), 255–265.

Houghton, J.T., Jenkins, G.J., Ephraums, J.J. (Eds.), 1990. Climate Change: the IPCC Scientific Assessment. Cambridge University Press, Cambridge, UK.

Huntley, B., 1988. In: Huntley, B., Webb III, T. (Eds.), Vegetation History. Glacial and Holocene vegetation history: Europe. Kluwer Academic Publishers, Dordrecht, ISBN 90-6193-188-6, 341–383.

Huntley, B., Prentice, I.C., 1988. July temperatures in Europe from pollen data, 6000 years before present. Science 241, 687–690.

Huntley, B., Prentice, I.C., 1993. In: Wright, H.E., Kutzbach, J.E., Webb III, T., Ruddiman, W.F., Street-Perrott, F.A., Bartlein, P.J. (Eds.), Global Climates since the Last Glacial Maximum. Holocene Vegetation and Climates of Europe. University of Minnesota Press, Minnesota, MN, pp. 136–168.

Hyvärinen, H., Alhonen, P., 1994. Holocene lake-level changes in the Fennoscandian tree-line region, western Finish Lapland: diatom and cladoceran evidence. The Holocene 4, 251–258.

Jones, P.D., Briffa, K.R., Barnett, T.P., Tett, S.F.B., 1998. High-resolution palaeoclimatic records for the last millennium: interpretation, integration and comparison with General Circulation Model control-run temperatures. The Holocene 8 (4), 455–471.

Jones, P.D., Osborn, T.J., Briffa, K.R., 2001. The evolution of climate over the last millennium. Science 292 (5517), 662–667.

Kallel, N., Paterne, M., Labeyrie, L., Duplessy, J.-C., Arnold, M., 1997. Temperature and salinity records of the Tyrrhenian Sea during the last 18,000 years. Palaeogeography, Palaeoclimatology, Palaeoecology 135, 97–108.

Karlén, W., 1988. Scandinavian glacial climatic fluctuations during the Holocene. Quaternary Science Reviews 7, 199–209.

Karlén, W., 1998. Climate variations and the enhanced greenhouse effect. Ambio 27, 270–274.

Korhola, A., Weckstrom, J., Holmstrom, L., Erasto, P., 2000. A quantitative Holocene climatic record from diatoms in northern Fennoscandia. Quaternary Research 54 (2), 284–294.

Korhola, A., Vasko, K., Toivonen, H.T.T., Olander, H., 2002. Holocene temperature changes in northern Fennoscandia reconstructed from chironomids using Bayesian modelling. Quaternary Science Reviews 21 (16–17), 1841–1860.

Kullman, L., 1995. Holocene tree-limit and climate history from the Scandes Mountains, Sweden. Ecology 768, 2490–2502.

Kutzbach, J.E., Webb III, T., 1993. In: Wright, H.E., Kutzbach, J.E., Webb III, T., Ruddiman, W.F., Street-Perrott, F.A., Bartlein, P.J. (Eds.), Global Climates since the Last Glacial Maximum. Conceptual Basis for Understanding Late-Quaternary Climates. University of Minnesota Press, Minnesota, MN, pp. 5–11.

Landmann, G., Reimer, A., 1996. Climatically induced lake level changes at Lake Van, Turkey, during the Pleistocene/Holocene transition. Global Biogeochemical Cycles 10 (4), 797–808.

Lauritzen, S.-E., Lundberg, J., 1999. Calibration of the speleothem delta function: an absolute temperature record for the Holocene in northern Norway. The Holocene 9 (6), 659–669.

Lou, Z., Wahba, G., Johnson, D.R., 1998. Spatial–temporal analysis of temperature using smoothing spline ANOVA. Journal of Climate 11 (1), 18–28.

Magny, M., 1993. Holocene fluctuations of lake levels in the French Jura and sub-Alpine ranges, and their implications for past general circulation patterns. The Holocene 3 (4), 306–313.

Magny, M., Guiot, J., Schoellammer, P., 2001. Quantitative reconstruction of Younger Dryas to mid-Holocene palaeoclimates at Le Locle, Swiss Jura, using pollen and lake-level data. Quaternary Research 56, 170–180.

Mann, M.E., Bradley, R.S., Hughes, M.K., 1999. Northern Hemisphere temperatures during the last millennium: inferences, uncertainties and limitations. Geophysical Research Letters 26, 759–762.

Marchal, O., Cacho, I., Stocker, T., Grimalt, J.O., Calvo, E., Martrat, B., Shackleton, N., Vautravers, M., Cortijo, E., van Kreveld, S., Andersson, C., Koç, N., Chapman, M., Sbaffi, L., Duplessy, J.-C., Sarnthein, M., Turon, J.-L., Duprat, J., Jasen, E., 2002. Apparent long-term cooling of the sea surface in the northeast Atlantic and Mediterranean during the Holocene. Quaternary Science Reviews 21, 455–483.

Masson, V., Cheddadi, R., Braconnot, P., Joussaume, S., Texier, D., PMIP participants., 1999. Mid-Holocene climate in Europe: what can we infer from PMIP model-data comparison? Climate Dynamics 15, 163–182.

Mauquoy, D., Barber, K., 1999. Evidence for climatic deteriorations associated with the decline of *Sphagnum imbricatum* Horsch. *ex* Russ. in six ombrotrophic mires from northern England and the Scottish Borders. The Holocene 9 (4), 423–437.

McDermott, F., Frisia, S., Huang, Y., Longinelli, A., Spiro, B., Heaton, T.H.E., Hawkesworth, C.J., Borsato, A., Keppens, E., Fairchild, I.J., van der Borg, K., Verheyden, S., Selmo, E., 1999. Holocene climate variability in Europe: evidence from $\delta^{18}O$, textural and extension-rate variations in three speleothems. Quaternary Science Reviews 18, 1021–1038.

McDermott, F., Mattey, D.P., Hawkesworth, C., 2001. Centennial-scale Holocene climate variability revealed by a high-resolution Speleothem $\delta^{18}O$ record from SW Ireland. Science 294, 1328–1331.

Mercone, D., Thompson, J., Croudace, I.W., Siani, G., Paterne, M., Troelstra, S., 2000. Duration of S1, the most recent sapropel in the eastern Mediterranean Sea, as indicated by accelerator mass spectrometry radiocarbon and geochemical evidence. Paleoceanography 15 (3), 336–347.

Moran, P.A.P., 1950. Notes on continuous stochastic phenomena. Biometrika 37, 17–23.

Myers, P.G., Rohling, E.J., 2000. Modeling a 200-yr interruption of the Holocene Sapropel S-1. Quaternary Research 53 (1), 98–104.

Nesje, A., Olaf Dahl, S., Andersson, C., Matthews, J.A., 2000. The lacustrine sedimentary sequence in Sygneskardvatnet, western Norway: a continuous, high-resolution record of the Jostedalsbreen ice cap during the Holocene. Quaternary Science Reviews 19, 1047–1065.

Nesje, A., Matthews, J.A., Olaf Dahl, S., Berrisford, M.S., Andersson, C., 2001. Holocene glacier fluctuations of Flatebreen and winter-precipitation changes in the Jostedalsbreen region, western Norway, based on glaciolacustrine sediment records. The Holocene 11 (3), 267–280.

Nicolussi, K., Patzelt, G., 2000. Discovery of early-Holocene wood and peat on the forefield of the Pasterze Glacier, Eastern Alps, Austria. The Holocene 10 (2), 191–199.

Nychka, D., Meiring, W., Royle, J.A., Fuentes, M., Gilleland, E., 2000. FIELDS: S tools for spatial data. Available at http://www.cgd.ucar.edu/stats/software.

Peyron, O., Guiot, J., Cheddadi, R., Tarasov, P., Reille, R., de Beaulieu, J.-L., Bottema, S., Andrieu, V., 1998. Climatic reconstruction in Europe for 18,000 yr BP from pollen data. Quaternary Research 49, 183–196.

Peyron, O., Jolly, D., Bonnefille, R., Vincens, A., Guiot, J., 2000. Climate of East Africa 6000 ^{14}C Yr B.P. as inferred from pollen data. Quaternary Research 54, 90–101.

Prentice, I.C., Guiot, J., Huntley, B., Jolly, D., Cheddadi, R., 1996. Reconstructing biomes from palaeoecological data: a general method and its application to European pollen data at 0 and 6 ka. Climate Dynamics 12, 185–194.

Prentice, I.C., Harrison, S.P., Jolly, D., Guiot, J., 1997. The climate and biomes of Europe at 6000 yr bp: comparison with model simulations and pollen-based reconstructions. Quaternary Science Reviews 17 (6–7), 659–668.

Reed, J.M., Stevenson, A.C., Juggins, S., 2001. A multi-proxy record of Holocene climatic change in southwestern Spain: the Laguna Medina, Cadiz. Holocene 11 (6), 707–719.

Roberts, N., Reed, J.M., Leng, M.J., Kuzucuoglu, C., Fontugne, M., Bertaux, J., Woldring, H., Bottema, S., Black, S., Hunt, E., Karabiyikoglu, M., 2001. The tempo of Holocene climatic change in the eastern Mediterranean region: new high-resolution crater-lake sediment data from central Turkey. Holocene 11 (6), 721–736.

Roca, J.R., Juliá, R., 1997. Late-Glacial and Holocene lacustrine evolution based on Ostracode assemblages in Southeastern Spain. Giobios 30 (6), 823–830.

Rohling, E.J., De Rijk, S., 1999. Holocene climate optimum and Last Glacial Maximum in the Mediterranean: the marine oxygen isotope record. Marine Geology 153, 57–75.

Rosén, P., Segerström, U., Eriksson, L., Renberg, I., Birks, H.J.B., 2001. Holocene climatic change reconstructed from diatoms, chironomids, pollen and near-infrared spectroscopy at an alpine lake (Sjuodjijaure) in northern Sweden. The Holocene 11 (5), 551–562.

Row III, L.W., Hastings, D., Dunbar, P., 1995. Terrain Base, Worldwide Digital Terrain Data, CD-ROM and Documentation Manual. NOAA, National Geophysical Data Center, Boulder, Colarado.

Seierstad, J., Nesje, A., Dahl, S.O., Simonsen, J.R., 2002. Holocene glacier fluctuations of Grovabreen and Holocene snow-avalanche activity reconstructed from lake sediments in Groningstolsvatnet, western Norway. The Holocene 12 (2), 211–222.

Seppä, H., Birks, H.J.B., 2001. July mean temperature and annual precipitation trends during the Holocene in the Fennoscandian tree-line area: pollen-based climate reconstructions. The Holocene 11 (5), 527–539.

Seppä, H., Birks, H.J.B., 2002. Holocene climate reconstructions from the fennoscandian tree-line area based on pollen data from Toskaijavri. Quaternary Research 572, 191–199.

Seppä, H., Nyman, M., Korhola, A., Weckstrom, J., 2002. Changes in tree-lines and alpine vegetation in relation to post-glacial climate dynamics in northern Fennoscandia based on pollen and chironomid records. Journal of Quaternary Science 17 (4), 287–301.

Shaopeng, H., Pollack, H.N., Po-Yu, S., 2000. Temperature trends over the past five centuries reconstructed from borehole temperatures. Nature 403(6771), 756–758.

Shemesh, A., Rosqvist, G., Rietta-Shati, M., Rubensdotter, L., Bigler, C., Yam, R., Karlén, W., 2001. Holocene climatic change in Swedish Lapland inferred from an oxygen-isotope record of lacustrine biogenic silica. The Holocene 11 (4), 447–454.

Terral, J.-F., Mengüal, X., 1999. Reconstruction of holocene climate in southern France and eastern Spain using quantitative anatomy of olive wood and archaeological charcoal. Palaeogeography, Palaeoclimatology, Palaeoecology 153, 71–92.

Tinner, W., Ammann, B., Germann, P., 1996. Treeline fluctuations recorded for 12,500 years by soil profiles, pollen and plant macrofossils in the Central Swiss Alps. Arctic and Alpine Research 28 (2), 131–147.

Vernet, J.-L., Pachiaudi, C., Bazile, F., Durand, A., Fabre, L., Heinz, C., Solari, M.-E., Thiébault, S., 1996. Le δ^{13}C de charbons de bois préhistoriques et historiques méditerranéens, de 35000 BP à l'actuel. Premier résultats. C. R. Acad. Sci. Paris Sér. IIs a t. 323, 319–324.

Weber, S.L., 2001. The impact of orbital forcing on the climate of an intermediate-complexity coupled model. Global and Planetary Change 30, 7–12.

Wick, L., Tinner, W., 1997. Vegetation changes and timberline fluctuations in the central airs as indicators of Holocene climatic oscillations. Arctic and Alpine Research 29 (4), 445–458.

Wilson, R.C.L., Drury, S.A., Chapman, J.L., 2000. The great ice age. Routledge, ISBN 0-415-19841-0, 267pp.

Yll, E.-R., Perez-Obiol, R., Pantaleon-Cano, J., Roure, J.M., 1997. Palynological evidence for climatic change and human activity during the Holocene on Minorca Balearic Islands. Quaternary Research 48, 339–347.

Zoller, H., Athanasiadis, N., Heitz-Weniger, A., 1998. Late-glacial and Holocene vegetation and climate change at the Palu glacier, Bernina pass, Grisons canton, Switzerland. Vegetation History and Archaeobotany 7 (4), 241–249.